Journal of Alzheimer's Disease 28 (2012) 403–422
DOI 10.3233/JAD-2011-111241
IOS Press

Monoamine Oxidase-A Physically Interacts with Presenilin-1(M146V) in the Mouse Cortex

Zelan Wei[a], Geraldine G. Gabriel[a], Lewei Rui[a], Xia Cao[a], Paul R. Pennington[a], Jennifer Chlan-Fourney[b], Adil J. Nazarali[c], Glen B. Baker[d] and Darrell D. Mousseau[a,*]
[a]*Cell Signalling Laboratory, Department of Psychiatry, University of Saskatchewan, Saskatoon, Canada*
[b]*Department of Anatomy and Cell Biology, University of Saskatchewan, Saskatoon, Canada*
[c]*Laboratory of Molecular Cell Biology, College of Pharmacy and Nutrition, University of Saskatchewan, Saskatoon, Canada*
[d]*Neurochemical Research Unit, Department of Psychiatry, University of Alberta, Edmonton, Canada*

Accepted 8 September 2011

Abstract. The concentration of presenilin-1 (PS-1) protein at the mitochondrial-associated aspect of the endoplasmic reticulum supports the potential for a mitochondrial influence of PS-1. Given that carriers of certain Alzheimer's disease (AD)-related PS-1 variants are predisposed to clinical depression and that depression has been historically associated with the mitochondrial enzyme, monoamine oxidase-A (MAO-A), we investigated cortical MAO-A function in the AD-related PS-1(M146V) knock-in mouse. The MAO-A system was clearly altered in the PS-1(M146V) mouse as revealed by (a) a mismatch between MAO-A protein expression and MAO-A activity; (b) changes in MAO-A-mediated monoaminergic neurotransmitter metabolism; (c) changes in non-cognitive behavior following treatment with the irreversible MAO-A inhibitor clorgyline; and (d) an increase in the potency of clorgyline in these same mice. We next investigated whether PS-1(M146V) could be influencing MAO-A directly. We observed (a) an enhanced MAO-A activity in necropsied PS-1(M146V) mouse cortical extracts incubated with DAPT (a PS-1 substrate-competitor); (b) the proximity of PS-1 with MAO-A and mitochondrial markers in cortical sections and in primary cortical neurons; (c) the co-segregation and co-immunoprecipitation of PS-1 and MAO-A within the mitochondrial fraction; and (d) the co-immunoprecipitation of overexpressed PS-1(M146V) and MAO-A proteins from N2a lysates. The PS-1(ΔEx9) and PS-1(D257A) variants, known to have low substrate-binding capacity, co-immunoprecipitated weakly with MAO-A. These combined data support a physical interaction between PS-1 and MAO-A that could influence MAO-A activity and contribute to the monoaminergic disruptions common to disorders as seemingly diverse as depression and AD.

Keywords: Alzheimer's disease, depression, mitochondria, monoamine oxidase, secretase

INTRODUCTION

The mitochondrial enzyme monoamine oxidase (MAO) degrades neurotransmitters such as serotonin and noradrenaline which are central to the neurobiology of depression [1, 2]. While the role of the MAO-B isoform in neurodegeneration has been widely studied [3], that of the MAO-A isoform (discussed below) is often considered ancillary to its well-established role in depression. However, aspects of depression and neurodegeneration could certainly rely on overlapping molecular mechanisms.

Alzheimer's disease (AD) is clinically characterized by a progressive loss of memory and executive

*Correspondence to: D.D. Mousseau, Cell Signalling Laboratory, B45 HSB, University of Saskatchewan, 107 Wiggins Rd., Saskatoon, SK (S7N 5E5), Canada. Tel.: +1 (306) 966 8824; E-mail: darrell.mousseau@usask.ca.

ISSN 1387-2877/12/$27.50

function, yet earlier stages of AD also present with non-cognitive symptoms including depression [4]. Depression might represent a prodrome for AD-related dementia in certain patients [5–7], with the rate of dementia increasing by 13% in a given patient for every hospital admission based on a depressive episode [8]. Given the acknowledged link between MAO-A and depression as well as the evidence that polymorphisms in the *MAO-A* promoter, particularly a variable number tandem repeat, have been linked to increased risk of developing depression [9] as well as AD [10–12], we hypothesized that MAO-A represents a commonality to depression and the early stages of AD. This is supported *a priori* by the accumulation in AD brains of toxic MAO-mediated metabolites [13] and with the early and progressive degeneration of serotonin neurons in the dorsal raphé nucleus and noradrenergic neurons in the locus coeruleus [14–18]. In late-onset AD, both MAO-A activity and mRNA have been shown to be elevated, although not necessarily concurrently, in cortical subregions, the locus coeruleus, thalamic nuclei, and white matter [19–22]. MAO-A activity has also been found to be decreased in late-onset AD brains [19, 23], but the 31% decrease in MAO-A activity in locus coeruleus is concomitant with a nearly 70–80% neuronal cell loss [19, 23, 24]. This suggests that the average MAO-A activity per *surviving* neuron is significantly increased [19]. In AD patients, monoaminergic tone is unequivocally affected [25] and MAO-A activity or the number of MAO-A immunoreactive neurons has also been implicated in cognitive decline [23]. A role for MAO-A in neurodegeneration is further supported by the observation that estrogen, a putative neuroprotective hormone, can selectively decrease MAO-A activity and mRNA levels *in vivo* [26, 27], whereas caspase-3-dependent apoptotic neuronal phenotypes following serum withdrawal or treatment with staurosporine are prevented by selective MAO-A inhibition [28, 29].

Recently, monoaminergic dysfunction in the context of AD has been associated with the presenilin-1 (PS-1)/γ-secretase pathway [30, 31]. The PS-1 protein is the catalytic core of the γ-secretase complex that processes the amyloid-β protein precursor to the amyloid-β (Aβ) 40- and 42-mer peptides [32, 33]. PS-1 has been associated with the mitochondria [34, 35], which supports an influence of PS-1 beyond the endoplasmic reticulum, one of its primary sites of action [36]. Furthermore, within the endoplasmic reticulum itself, presenilins are heterogeneously distributed, with a significant protein density being found in the membrane subcompartment at the interface with the mitochondria, aptly called the mitochondria-associated membrane (MAM) [37]. Given that protein contacts at the MAM facilitate communication and metabolic exchange between these two organelles [38], it is reasonable to consider that PS-1 could functionally influence mitochondrial-expressed proteins, including MAO.

A link between PS-1 and depression is strongly suggested by the finding that pre-demented carriers of the PS-1(A431E) and PS-1(L235V) variants are more likely to suffer from depression than non-carrier siblings (*note*, the fact that the carriers are pre-demented and unaware of their genotype excludes any possibility that their depression is reactive or secondary to a diagnosis of dementia/AD) [39]. Furthermore, in transgenic animal models of AD-related pathology, the antidepressants imipramine, citalopram, and rolipram (also a phosphodiesterase inhibitor) affect γ-secretase-mediated substrate processing as well as improve non-cognitive behavior *via* PS-1/γ-secretase-sensitive mechanisms [40, 41]. In addition, the *AβPPSwe/PS-1(M146V)* mouse model of amyloidosis exhibits changes in monoaminergic tone [42] and non-cognitive behaviors [43], and the *AβPPSwe/PS-1(ΔEx9)* mouse exhibits a substantial monoaminergic neurodegeneration, particularly in serotonergic and noradrenergic systems [30, 31]. The latter occurs independently of accumulation of either Aβ or phosphorylated tau protein [30]. Thus monoaminergic insult appears to represent an early event in AD-related pathology.

Given the interest in placing the mitochondrion as a pivotal component in the early stages of AD progression [44], the changes in monoaminergic function in experimental and clinical AD, and the link between PS-1 variants and depression, it is important to define the role for MAO in this context. We now provide data that support PS-1(M146V) as a negative regulator of MAO-A function in the sensorimotor cortex, a region affected during the progression of clinical AD [45]. Furthermore, subcellular fractionation, confocal microscopy, and co-immunoprecipitation experiments provide strong evidence that MAO-A interacts directly with PS-1 proteins. Mutations in the *PSEN-1* gene primarily account for the early-onset form of AD and fewer than 10% of all cases of AD. However, there is evidence that a mutation in *PSEN-1*, e.g., the one coding for the R249H substitution [46], is associated with the more common late-onset form of AD. Thus our demonstrated interaction between PS-1 and MAO-A could provide an explanation for a subtle role for PS-1 in non-cognitive neuropsychiatric disorders such as

depression. By extension, an influence of PS-1 on MAO-A function could also account for the ambiguity surrounding the role of MAO-A in both early-onset and late-onset AD-related pathology. Further characterization of this interaction in PS-1- and MAO-A-dependent pathologies is clearly warranted.

MATERIALS AND METHODS

Reagents and antibodies

5-Hydroxytryptamine (5-HT), N-[N-(3, 5-difluorophenacetyl)-L-alanyl]-S-phenylglycine *t*-butyl ester (DAPT) and the β-actin and FLAG antibodies were purchased from Sigma-Aldrich (Oakville, ON, Canada). [^{14}C]-5-HT (NEC-225) was purchased from PerkinElmer Life Sciences (Waltham, MA, USA). The MAO-A (H-70/T-19) and c-myc (A14) antibodies were purchased from Santa Cruz Biotechnology (Santa Cruz, CA, USA). The PS-1 antibody (MAB5232: loop region, residues 263–378) and the IP3R3 (AB9076) antibody were from Millipore/Chemicon (Temecula, CA, USA). The VDAC antibody was from EMD Biosciences (La Jolla, CA, USA), whereas the cytochrome c antibody (#556433) was from BD Pharmingen (Mississauga, ON, Canada). The PDI antibody (#3501) and the PS-1 antibody (#5643: D39D1 clone, carboxy terminus) were purchased from Cell Signalling Technology (Danvers, MA, USA). IgG-HRP conjugates were from Cedarlane Laboratories Ltd. (Burlington, ON, Canada). Mitotracker® Red was purchased from Invitrogen Canada Inc. (Burlington, ON, Canada).

The Psen1(M146V) mouse model of AD-related presenilin dysfunction

B6.129-Psen1^{tm1Mpm}/J PS-1 knock-in mice (The Jackson Laboratory; Bar Harbor, ME, USA) were originally generated by substitution of exon5 of the murine *Psen-1* gene for the homologous exon from human *PSEN-1*. The human exon specifically contained a double mutation that encoded for the I145V/M146V substitution, thereby not only introducing the AD-related M146V substitution, but also 'humanizing' the only amino acid polymorphism between mouse *Psen-1* and human *PSEN-1* genes (i.e., by introducing the I145V substitution). These mice express the corresponding humanized autosomal-dominant AD-related PS-1(M146V) protein at normal levels [47] and are routinely used to study aspects of PS-1/γ-secretase dysfunction in the context of AD-related pathology [47–49]. In all experiments, PS-1(M146V) mice were compared with their wildtype (WT) littermates. Mice were treated in accordance with the University Committee on Animal Care and Supply/Canadian Council on Animal Care guidelines.

Immunodetection and immunoprecipitation

Standard Western/SDS-PAGE denaturing conditions were used to detect expression of targeted proteins (precleared; 12,000 × g, 10 min, 4°C; 20–30 μg/lane) or in immunoprecipitates (200–500 μg) precipitated with protein-A/G Sepharose [50]. For immunoprecipitation experiments, non-specific binding to immunoglobulin (IgG) was avoided by preclearing lysates with an excess of normal mouse or rabbit IgG. Furthermore, immunoprecipitation reactions using non-specific IgG were included in each experimental run. Detection relied on enhanced chemiluminescence and all blots are representative of ≥3 individual experiments. ImageJ 1.32j (http://rsb.info.nih.gov/ij/) was used for densitometric analyses of scanned blots.

Quantitative real-time PCR

Total RNA was isolated using an RNeasy® Mini Kit (Qiagen; Mississauga, ON, Canada) and reverse-transcribed to cDNA using SuperScript™ RNase H-Reverse Transcriptase (Invitrogen). Gene expression was quantified using the Taqman® primers and labeled probe system, and a real-time thermocycler (ABI 7300), all from Applied Biosystems (Foster City, CA, USA). Reactions were performed using the Taqman Universal Master Mix (2X), FAM-labeled Taqman Gene Expression assays for the target gene, VIC-labeled Taqman Endogenous Control β-Actin, and 10 ng of cDNA. Thermocycling parameters were as follows: 2 min at 50°C, 10 min at 95°C, 40 cycles of 15 s at 95°C/70 s at 60°C. Taqman gene expression assays have all been tested to have efficiencies not significantly different from '1' (Applied Biosystems). To avoid variability in amplification efficiencies due to potential multiplexing of the gene-specific and β-actin primers, the primer sets were examined individually and in complex with β-actin. Standard curve reactions were run using 1, 10, and 100 ng of cortical cDNA and amplification efficiency was required to be between 90–110% for both the gene-specific and β-Actin primers sets [51]. All comparisons ($n = 3$–5, with four replicates) were performed using

quantification software (Applied Biosystems). The data were normalized to WT expression.

Monoamine oxidase (MAO) activity

MAO-A activity was estimated using 250 μM [^{14}C]-5-HT and 100 μg cell protein/reaction [52]. The reaction (10 min) was terminated by acidification and the labeled metabolites were extracted into ethyl acetate/toluene (1 : 1 vol/vol, water-saturated), an aliquot of which was subjected to scintillation spectrometry to determine radioactive content. All activity data represent 6 or more experiments, with each experiment performed in triplicate-quintuplicate.

Immortalized and primary neuronal cells

The mouse neuroblastoma N2a cell line (CCL-131) was obtained from American Type Culture Collection and maintained in 5% CO_2 at 37°C according to their specifications. Primary cortical neuronal cultures were prepared from E16.5 fetuses [53]. Neurons from WT and PS1(M146V) mouse fetuses were plated on coverslips (coated with 25 μg/ml poly-D-lysine) and grown in NeuroBasal medium with B27 supplement at 37°C with 5% CO_2-humidified atmosphere. Neurons (DIV 10) were fixed with 4% paraformaldehyde in 0.01 M PBS for 20 min at room temperature, washed several times with PBS, and used for immunofluorescence staining of PS-1, MAO-A and specific organelle markers, and the signals were detected by confocal microscopy.

Immunohistochemistry and fluorescence microscopy

Animals were perfused with 0.01 M PBS (pH 7.4). Brains were post-fixed in paraformaldehyde (4%: 24 h), transferred to cryoprotectant (30% glycerol/0.01 M PBS, 48 h), and stored at −70°C until sectioned (30 μm, coronally). The sections were then stored (25% glycerol; 25% ethylene glycol; 0.1 M PBS) at 4°C until processed.

DAB-immunohistochemistry was performed on free-floating sections that had been rinsed in 0.01 M PBS, treated with 0.2% H_2O_2 in 0.01 M PBS (30 min) and blocked in 5% normal serum in PBS containing 0.2% Triton (PBS-TX) (1.5 h). Sections were then incubated (4°C, 72 h) with the rabbit polyclonal H-70 MAO-A antibody (1 : 100) in 5% normal serum-PBS-TX. Sections were incubated with biotinylated goat anti-rabbit (BA-1000, Vector Laboratories Canada; Burlington, ON, Canada) (1 : 250, 1.5 h) and processed by the ABC-DAB method. All steps were followed by washes in PBS (3 × 20 min). The sections were also processed for thionin/Nissl staining. Sections were mounted on gelatin-coated slides, dehydrated in ascending alcohols, cleared with xylene, and coverslipped with ProLong® Gold (Invitrogen) for visualization using a BX-51 microscope system (Olympus Canada; Markham, ON, Canada). All experiments included control sections incubated in the absence of primary antibody (data not shown).

The distribution of PS-1 in primary cortical cultures was compared to the distribution of MAO-A, VDAC, and IP3R3 using a 63X water immersion lens on a ZEISS LSM 510 Confor2 confocal microscope and AxioVision Rel. 4.8 software. Fixed primary cultures (on coverslips) were blocked in 5% normal horse serum in PBS containing 0.3% Triton-100 (PBS-TX) (30 min) and then processed for double immunofluorescence with anti-PS-1 (goat polyclonal; 1 : 250) paired with each of the following antibodies: the MAO-A H70 antibody (1 : 250); mouse monoclonal VDAC (1 : 250); or rabbit polyclonal IP3R3 (1 : 250). Secondary antibodies (1 : 250) were applied as described above and included Alexa Fluor® (Invitrogen) 488 donkey-anti-goat with either 594 donkey-anti-mouse or donkey-anti-rabbit.

The localization of PS-1 and MAO-A in the cortex of 6-month old WT and PS-1(M146V) mice was visualized in a similar manner. Free-floating sections (30 μm) were treated for antigen retrieval in sodium citrate buffer for 30 min at 70°C, blocked in 5% normal serum, and then placed in primary (1 : 100) and secondary (1 : 500) antibody solution as described above. All experiments included control sections incubated in the absence of primary antibody (data not shown). Where indicated, thin optical sections were used for confocal images, with each optical section in the z-axis being <1.0 μm. In all cases, images from the three transmission channels (e.g., the Ar, HeNe1, and Diode lasers) were captured sequentially.

Subcellular fractionation

Enriched endoplasmic reticulum (ER) and mitochondrial fractions were obtained [37, 54] from fresh cortices harvested from 6-month old WT and PS-1(M146V) mice. Briefly, cortices were homogenized gently in isolation buffer-1 (250 mM mannitol, 5 mM HEPES pH 7.4, and 0.5 mM EGTA) with four strokes in a loose Potter-Elvehjem grinder. The heavy membrane fraction (cell debris and nuclei)

was removed (2 × 5 min; 750 × g) and the supernatant was centrifuged (10 min; 9,000 × g); this separated the ER/microsomal fraction (supernatant) from the crude mitochondrial fraction (P2 pellet). The ER fraction was centrifuged (30 min; 20,000 × g) to get rid of lysosomal and plasma membrane contaminants, and the resultant supernatant was centrifuged (1 h; 100,000 × g). The pellet represents the ER-enriched fraction and the supernatant represents the cytosolic fraction. The P2 pellet was resuspended in isolation buffer-2 (isolation buffer-1 lacking EGTA) and centrifuged (10 min; 10,000 × g). It was resuspended in isolation buffer-3 (isolation buffer-2 lacking BSA) and centrifuged again (10 min; 10,000 × g) to obtain the crude mitochondrial pellet. Note that the mitochondria and MAM co-fractionated with this differential centrifugation protocol. All fractions were quantitated for protein prior to Western blot analysis.

Non-cognitive/behavioral assay

Alterations in non-cognitive behaviors have been reported in the AβPP*Swe*/PS-1(M146V) mouse [43]. We chose to examine the role of MAO-A on non-cognitive behavior in 6 month-old PS-1(M146V) mice by using the Forced-Swim Test (FST), which models behavioral despair and was originally developed for the screening of antidepressants [55]. Clorgyline (CLG) is a selective, irreversible inhibitor of MAO-A with antidepressant potential [56, 57]. Although CLG's irreversibility precipitates hypertensive crises and, thus, limits its use in the clinic, it is its irreversibility that validates it as a pharmacological tool for studying MAO-A function.

Mice were placed in a glass cylinder (46 cm high × 20 cm Φ) of water (∼24°C) filled to a depth of 30 cm, thus preventing the mice from resting on the bottom of the cylinder. Water was changed between test runs. Treatments [saline or CLG (1 mg/kg), $n = 6$–9] were administered 2 h prior to a 6-min test swim (includes a pre-exposure period of 2 min followed by a 4-min test session immediately thereafter). This dose-regimen of CLG was chosen as it does not affect either immobility time in the FST [58] or ambulatory behavior [59] in WT mice, but it does affect the tissue content of monoaminergic neurotransmitters [59].

High pressure liquid chromatography (HPLC)

Mice were sacrificed and brains were regionally dissected, snap-frozen and stored at −70°C until processed for neurochemical correlates [60]. HPLC was performed using a Waters instrument and pumps, a Bioanalytical Systems (West Lafayette, IN, USA) LC-4B amperometric detector and a Hewlett-Packard (Palo Alto, CA, U.S.A.) 3392A integrator. The compounds of interest were measured using a glassy carbon electrode set at 0.75 V *versus* an Ag/AgC1 reference electrode. The flow rate was 1 ml/min through a C18 column (4.6 mm × 250 mm; 5 μm particle size, Applied Science Labs, Avondale, PA, USA) coupled to a precolumn. The mobile phase consisted of NaH_2PO_4 (55 mM), sodium octyl sulfate (0.85 mM), disodium EDTA (0.37 mM) and acetonitrile (9%) and was filtered, degassed, and adjusted to pH 3.0. The concentrations of analytes were determined by comparing peak height ratios to those of a set of authentic standards processed in parallel.

Expressions plasmids and transient transfections

Wildtype PS-1 cDNA [61] was obtained from Dr. G. Lévesque (Université Laval, Québec, Canada) and served as a template for targeted substitutions (QuikChange®, Stratagene). Cells in log-phase were transfected (50% efficiency) with cDNA (i.e., 1–2 μg/well on a 24-well plate; seeded at 5×10^5 cells/well) using LipoFectamine2000 (Invitrogen). Cells were routinely harvested 24 h post-transfection.

Statistical analyses

Significance was set at $p < 0.05$ and assessed by unpaired *t*-tests or by ANOVA with *post hoc* analyses relying on Bonferroni's Multiple Comparison Test (GraphPad Prism v3.01). Data are represented as mean ± standard error of the mean (SEM).

RESULTS

Our research program focuses on the post-translational regulation of MAO function in several mouse models of AD-related pathology. We now report our findings from the PS-1(M146V) knock-in mouse, which is used routinely to study AD-related PS-1/γ-secretase function.

MAO-A protein is induced in a PS-1(M146V) background

Western blot revealed an increase in MAO-A expression in cortical extracts of 6-month old PS-1(M146V) mice (Fig. 1A). This was confirmed by densitometry (+∼50%) [$t = 3.168$, df = 8, $p = 0.0132$] (Fig. 1B).

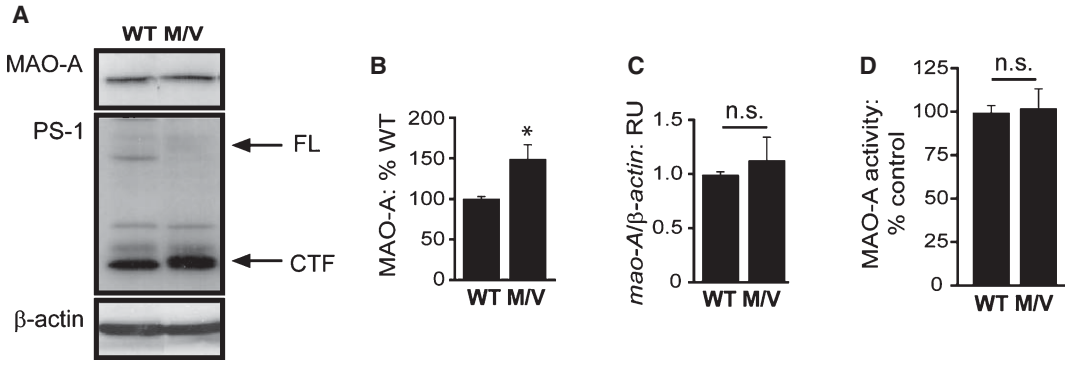

Fig. 1. MAO-A protein expression does not reflect activity in the PS-1(M146V) knock-in mouse cortex. A) Western blot was used to examine cortical extracts of 6-month old PS-1(M146V) (M/V) mice (compared to age-matched WT littermates) for MAO-A expression and for the full length (FL) PS-1 and the ~20 kDa PS-1 C-terminal fragment (CTF). B) Densitometric analysis ($n = 5$, mean ± SEM) confirms the increase in MAO-A expression in cortical extracts from PS-1(M146V) mice. C) Quantitative real-time PCR determination of *mao-A* mRNA expression, normalized to *β-actin* mRNA expression, in WT and PS-1(M146V) cortex (RU: relative units; $n = 3$–5, mean ± SEM). D) MAO-A activity (mean ± SEM, $n = 5$-6) was assayed in corresponding cortical extracts. n.s.: not significant.

The full-length PS-1 protein was barely visible in PS-1(M146V) extracts, but accumulation of the ~20 kDa C-terminal fragment was evident (Fig. 1A). β-actin expression demonstrated equal protein loading. *mao-A* mRNA levels (qRT-PCR) were not affected by the PS-1(M146V) knock-in [$t = 0.446$, df = 6, $p = 0.6713$] (Fig. 1C). We assayed corresponding homogenates for MAO-A activity and found that the increase in MAO-A protein expression in PS-1(M146V) mouse cortex was not reflected by a concomitant increase in MAO-A activity [$t = 0.250$, df = 14, $p = 0.8060$] (Fig. 1D).

Immunohistochemistry reveals differences in MAO-A distribution and laminar organization in sensorimotor cortex of PS-1(M146V) mice

In 6-month old WT mice, MAO-A DAB-immunoreactivity was observed throughout the neuropil of cortical layers I-VI, with increased immunoreactivity observed in and around cell bodies of layer II, superficial layer III, and layer V (Fig. 2A). In contrast, MAO-A immunoreactivity in PS-1(M146V) mice (Fig. 2D) was detected in patches throughout the entire neuropil. Thionin (Nissl) staining [at 10X (Fig. 2B, E) and 4X (Fig. 2C, F) magnification] also revealed an abnormal patchy distribution of Nissl substance and disrupted laminar boundaries in the PS-1(M146V) cortex. Immunofluorescence microscopy confirmed the induction of MAO-A in cell soma and neuropil of the PS-1(M146V) mouse cortex (Fig. 2G, H).

These data (Figs. 1 and 2) indicate a mismatch between MAO-A protein and catalytic activity in the PS-1(M146V) mouse cortex. This discrepancy between levels of MAO-A protein and activity (Figs. 1-2) is not novel [50, 52, 62–64] and further supports the potential for post-translational regulation of MAO-A function. It is clear that the MAO-A system is affected in the PS-1(M146V) mouse cortex. We chose to examine next how *in vivo* MAO-A inhibition would affect behavioral and neurochemical correlates in the PS-1(M146V) mouse.

MAO-A inhibition affects non-cognitive behavior in the PS-1(M146V) mouse

Six month-old WT and PS-1(M146V) mice were treated acutely with the PBS vehicle or the selective MAO-A inhibitor clorgyline (CLG: 1 mg/kg, i.p., 2 h) and subjected to the FST. Treatment with CLG did not elicit any behavioral effect in WT mice, as expected [59], but it did decrease the amount of time that their PS-1(M146V) littermates spent swimming [$F_{(3,24)} = 3.425$, $p = 0.0359$] (Fig. 3). Although this was not the anticipated response for an antidepressant drug, this was not entirely unexpected as MAO inhibitors do not always increase the 'swim time' in the FST [65]. Western blot demonstrated that MAO-A expression was not affected by CLG treatment (Fig. 3).

Brain levels of aminergic neurotransmitters are affected in the PS-1(M146V) mouse

We used HPLC to measure the levels of neurotransmitters in corresponding WT and PS-1(M146V) cortical extracts. Analytes included dopamine (DA), NA,

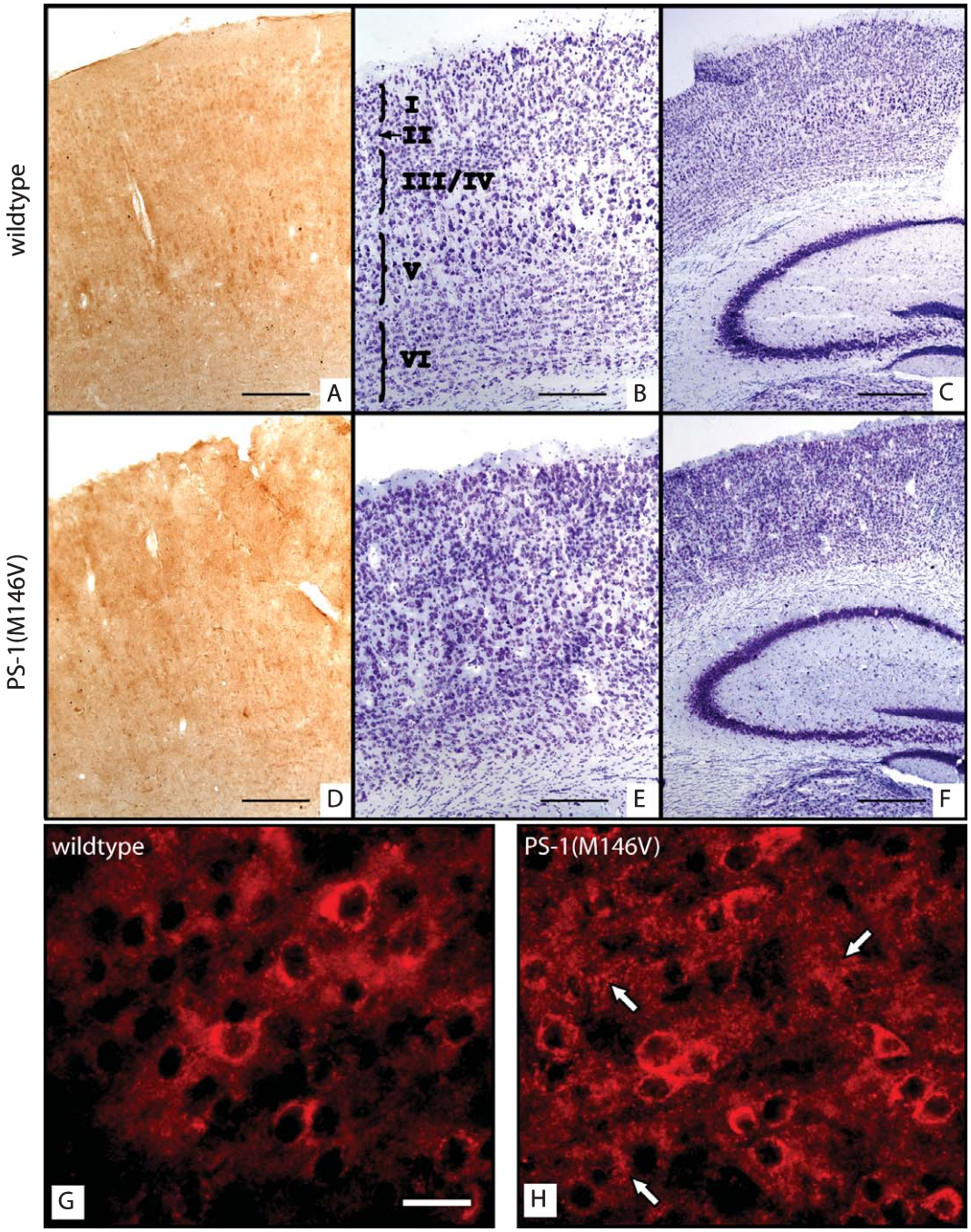

Fig. 2. MAO-A immunoreactivity and thionin staining in WT and PS-1(M146V) mouse sensorimotor cortex. Coronal sections of 6-month old WT (A, B, C) and PS-1(M146V) (D, E, F) mice were used for DAB-MAO-A immunohistochemistry (A, D) and Nissl staining (B, C, E, F). Scale bars = 125 μm (A, B, D, E) and 500 μm (C, F). Immunofluorescence confirms (G) detection of MAO-A in the WT mouse cortex and (H) the induction of the MAO-A protein in the PS-1(M146V) cortex. In (H) the appearance of numerous, extracellular punctate MAO-A-immunoreactive signals (white arrows) undoubtedly account for the patchy distribution seen with DAB-MAO-A immunohistochemistry (D) in the same mice. Scale bar = 20 μm.

and 5-HT, and selected acid metabolites [DOPAC: 3, 4-dihydroxyphenylacetic acid; HVA: homovanillic acid; 5-HIAA: 5-hydroxyindolacetic acid] (Fig. 4). The statistics for the various analytes were as follows: 5-HT [$F_{(3,36)} = 12.99$, $p < 0.0001$], 5-HIAA [$F_{(3,39)} = 18.95$, $p < 0.0001$], DA [$F_{(3,30)} = 2.266$, $p = 0.1035$], DOPAC

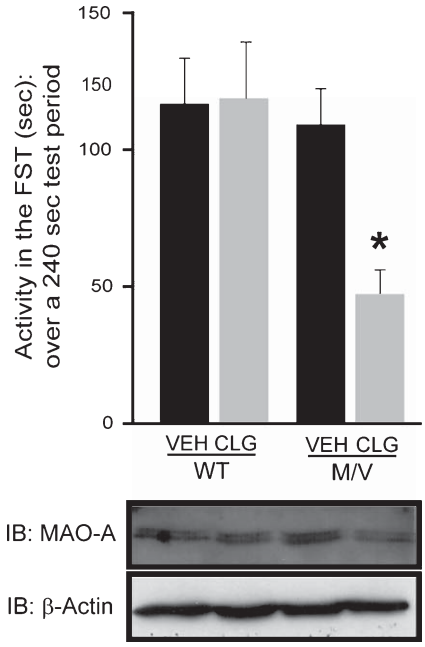

Fig. 3. MAO-A-sensitive non-cognitive behavior is affected in the PS-1(M146V) mouse. 6-month old PS-1(M146V) mice (M/V) and WT littermates were treated with either saline vehicle (VEH) or the selective MAO-A inhibitor clorgyline (CLG; 1 mg/kg, 2 h) and then tested using the Forced Swim Test (FST). Western blot analysis depicts MAO-A protein expression in corresponding cortical extracts and β-actin demonstrates equal protein loading. $^{*}p<0.05$ versus VEH-treated M/V group ($n=6$–8, mean ± SEM).

[$F_{(3,33)}=5.540$, $p=0.0041$], HVA [$F_{(3,37)}=6.528$, $p=0.0013$] and NA [$F_{(3,38)}=5.017$, $p=0.0054$]. *Post hoc* analyses revealed that PS-1(M146V) expression exerted changes in amine and metabolite levels that resemble characteristic MAO inhibition, i.e., amine levels increase while corresponding metabolite (DOPAC and 5-HIAA) levels decrease. Acute treatment with CLG exerted changes in cortical catecholamine metabolism, but did not affect the levels of 5-HT or 5-HIAA (Fig. 4).

The potency of CLG is altered in the PS-1(M146V) cortex

MAO-A activity in cortical homogenates from mice (used for Figs. 3 and 4) confirmed that the dose-regimen with CLG inhibited MAO-A activity, but also revealed that CLG was more potent in a PS-1(M146V) background [$F_{(3,18)}=20.02$, $p<0.0001$] (Fig. 5). CLG dose-response curves ($n=4$) using WT [$R^2=0.9987$] and PS-1(M146V) [$R^2=0.9988$] mouse cortical homogenates revealed logIC_{50} values (μM) of −2.385 (±0.073) and −1.946 (±0.045), respectively. Although this was statistically significant [$t=11.44$, df = 6, $p<0.0001$], it is not a pharmacologically substantial shift in the response curve (Fig. 5). The respective Hill coefficients were −0.827 (±0.084) and

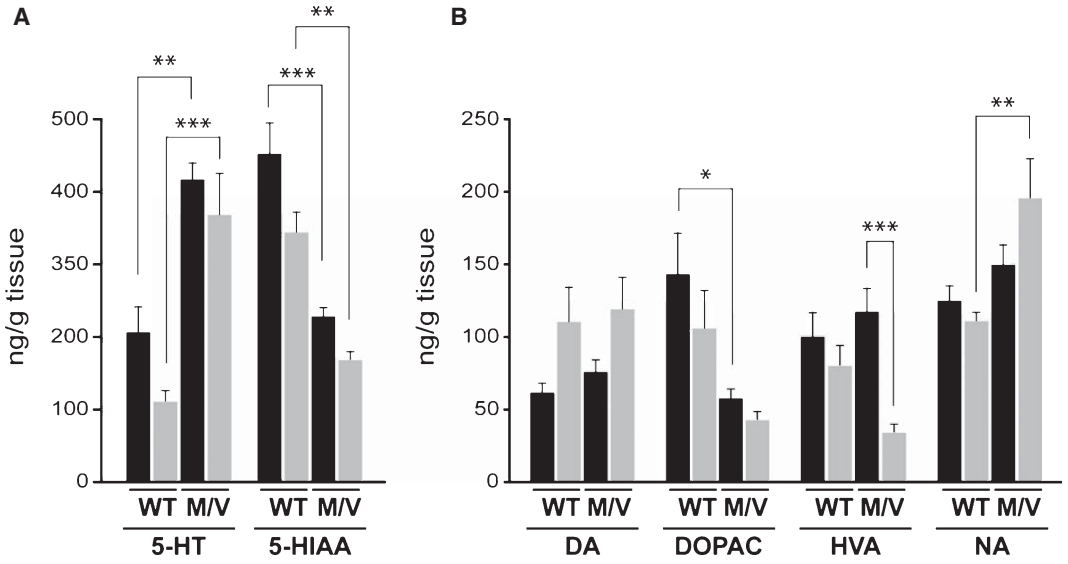

Fig. 4. Cortical aminergic analytes are affected by expression of the PS-1(M146V) variant. Neurochemical analyses were performed on cortical extracts from the mice used in the FST (see Fig. 3). A) Levels of serotonin (5-HT) and its acid metabolite 5-HIAA were measured in saline-treated (black bars) or CLG-treated (grey bars) mice. $^{**}p<0.01$, $^{***}p<0.001$, between indicated groups (mean ± SD, $n=7$–13). B) Levels of dopamine (DA), and its two acid metabolites DOPAC and HVA, as well as that of noradrenaline (NA) were also measured. $^{*}p<0.05$; $^{**}p<0.01$, $^{***}p<0.001$, between indicated groups ($n=8$–13, mean ± SEM).

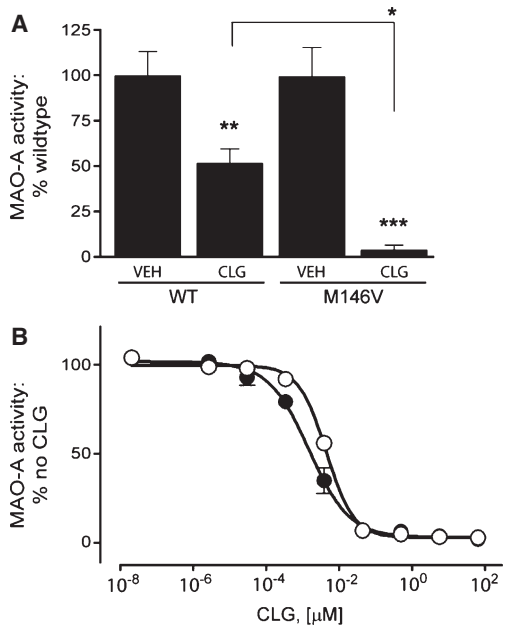

Fig. 5. The potency of CLG is increased by the PS-1(M146V) variant *in vivo*. A) MAO-A activity was examined in cortical extracts from PS-1 WT or PS-1(M146V) animals used for behavioural and neurochemical analyses in Figs. 3–4 ($n = 6$, mean ± SEM). B) CLG concentration-response curves were generated using cortical extracts from vehicle-treated WT (•) and PS-1(M146V) (○) animals. $^{*}p < 0.05$, $^{**}p < 0.01$, $^{***}p < 0.001$, versus vehicle (veh)-treated WT control or between indicated groups ($n = 4$–6, mean ± SEM).

−1.209 (±0.187) [$t = 3.734$, df = 6, $p = 0.0097$], which does suggest a change in cooperativity.

These data (Figs. 3–5) suggest that the PS-1(M146V) variant affects monoaminergic tone and predisposes to MAO-A-sensitive behavior, and that this is potentially due to non-canonical effects on the MAO-A protein itself.

The PS-1/γ-secretase inhibitor DAPT enhances MAO-A activity in necropsied PS-1(M146V) mouse cortical homogenates and suggests a direct role for PS-1 in MAO-A function

We used a pharmacological approach to investigate whether the effects of PS-1(M146V) on MAO-A function could be due to a direct influence of this variant on the MAO-A protein. We pre-incubated (10 min) homogenates of *necropsied* cortices from both WT and PS-1(M146V) littermates with increasing concentrations of DAPT, a γ-secretase substrate-competitive inhibitor [66]. Note that the use of necropsied brain samples precluded any possibility of *de novo* protein synthesis. MAO-A activity was increased by DAPT in a concentration-dependent manner in PS-1(M146V) mouse homogenates [$F_{(5,17)} = 5.945$, $p = 0.005$], but not in WT mouse homogenates [$F_{(5,17)} = 1.128$, $p = 0.397$] (Fig. 6A), which strongly suggests that DAPT was interfering with an endogenous interaction between PS-1(M146V) and MAO-A. The Effective Concentration required to induce a 50% effect (EC_{50}) for the *in vitro* activation of MAO-A by DAPT was estimated using the effect at 0 nM (0%: control) and at 10,000 nM as minima and maxima ($n = 4$). Linear regression analysis revealed an EC_{50} of 161.1 nM [95% CI: 136.2 to 190.6 nM; $R^2 = 0.999$], which is similar to the low nM IC_{50} values reported for DAPT-mediated inhibition of well-known γ-secretase interactions, i.e., with AβPP, *in vitro* [66, 67]. In addition, the fact that the PS-1 inhibitor, DAPT, can *induce* MAO-A activity supports our initial conclusion that PS-1(M146V) negatively regulates MAO-A function *in vivo*.

The expression of PS-1 and MAO-A are in close proximity in mouse cortical sections

Confocal microscopic examination of the sensorimotor cortex of 6 month-old WT and PS-1(M146V) mice revealed a diffuse distribution of PS-1 throughout the neuronal cytoplasm (Fig. 6B). The distribution of MAO-A was affected by the expression of PS-1(M146V) and while still detected in the cell soma, it also presented a punctate distribution in the neuropil (as already observed in Fig. 2). The overlap between the two signals in WT sections was modest (Fig. 6C). In contrast, in the PS-1(M146V) sections, the MAO-A signal was stronger and the overlap between the PS-1 and MAO-A signals was more evident (Fig. 6C).

The localization of PS-1 to the mitochondrial compartment supports a direct role for PS-1 in MAO-A function

Confocal microscopy of primary cortical neurons revealed that PS-1 immunoreactivity overlaps regions that are also positive for MAO-A as well as for the voltage-dependent anion channel (VDAC; a known marker of the outer mitochondrial membrane) and for IP3R3 (a marker of the MAM of the ER: [68]) (Fig. 7). The proximity of PS-1 to the mitochondrial/MAM compartment supports the potential for a physical interaction between PS-1 and MAO-A.

Fractionation studies confirmed the association of PS-1 with the ER-enriched fraction as well as a modest MAO-A signal in this same fraction (Fig. 8). Yet, both immunofluorescence and Western

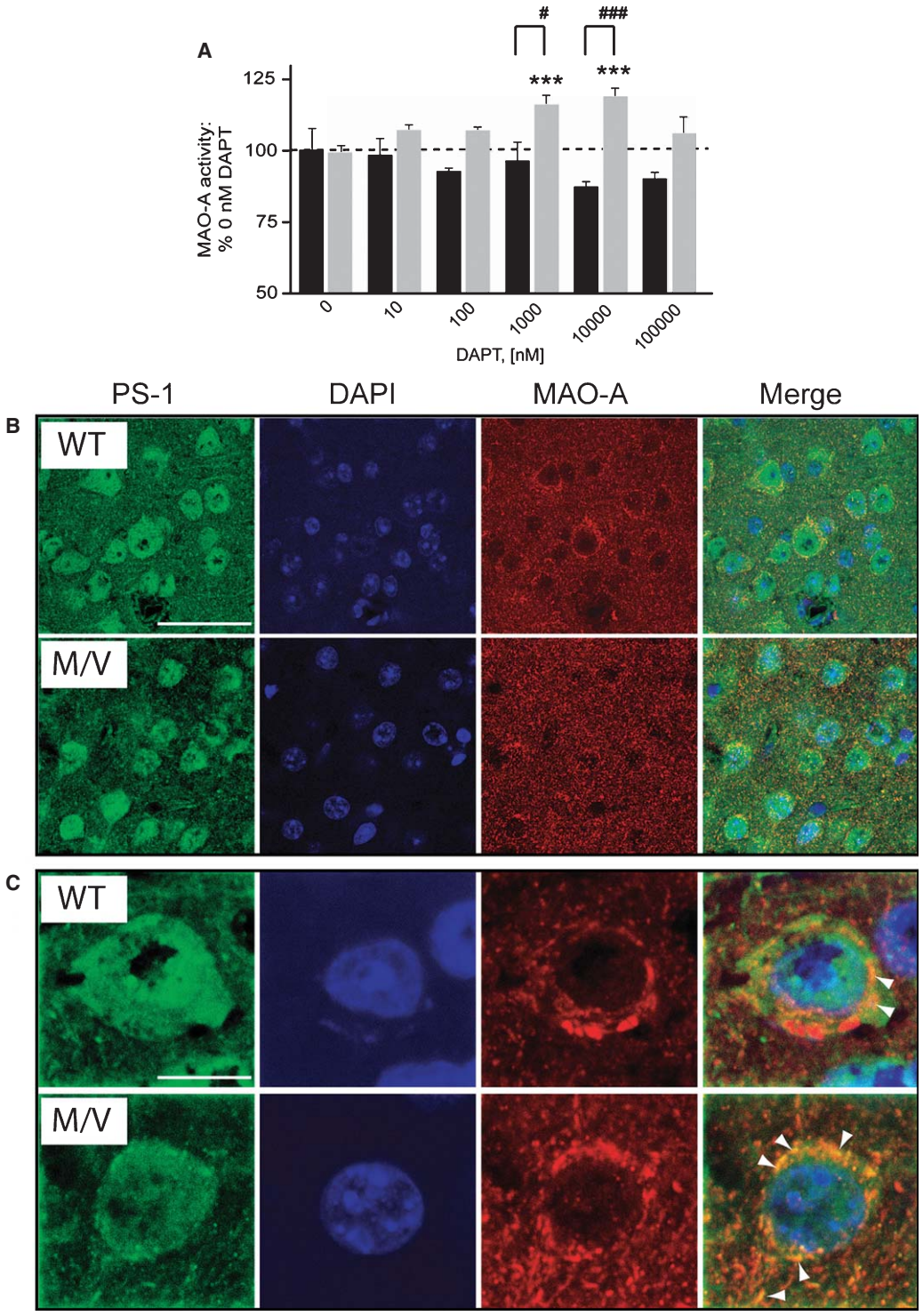

Fig. 6. Pharmacology and microscopy suggest that PS-1 and MAO-A are expressed in close proximity *in vivo*. A) Cortical homogenates from 6-month-old WT (black bars) or PS-1(M146V) mice (grey bars) were assayed for MAO-A activity in the presence of increasing concentrations of the PS-1/γ-secretase competitive substrate inhibitor DAPT. $^{***}p < 0.001$ versus the corresponding [0 nM] control group; $^{\#}p < 0.05$, $^{\#\#\#}p < 0.001$ between indicated groups. B) Laser-scanning confocal microscopy reveals that PS-1 (red) and MAO-A (green) can both be detected in close proximity in certain cells (merged, yellow). Cell nuclei were counterstained with DAPI (blue). Scale bar = 40 μm. C) Cells were examined at higher magnification (scale bar = 8 μm). In the merged image, areas that are strictly PS-1-positive (green) or MAO-A-positive (red) are clearly evident as are areas of overlap (merge, yellow: arrowheads) in both the cell and neuropil.

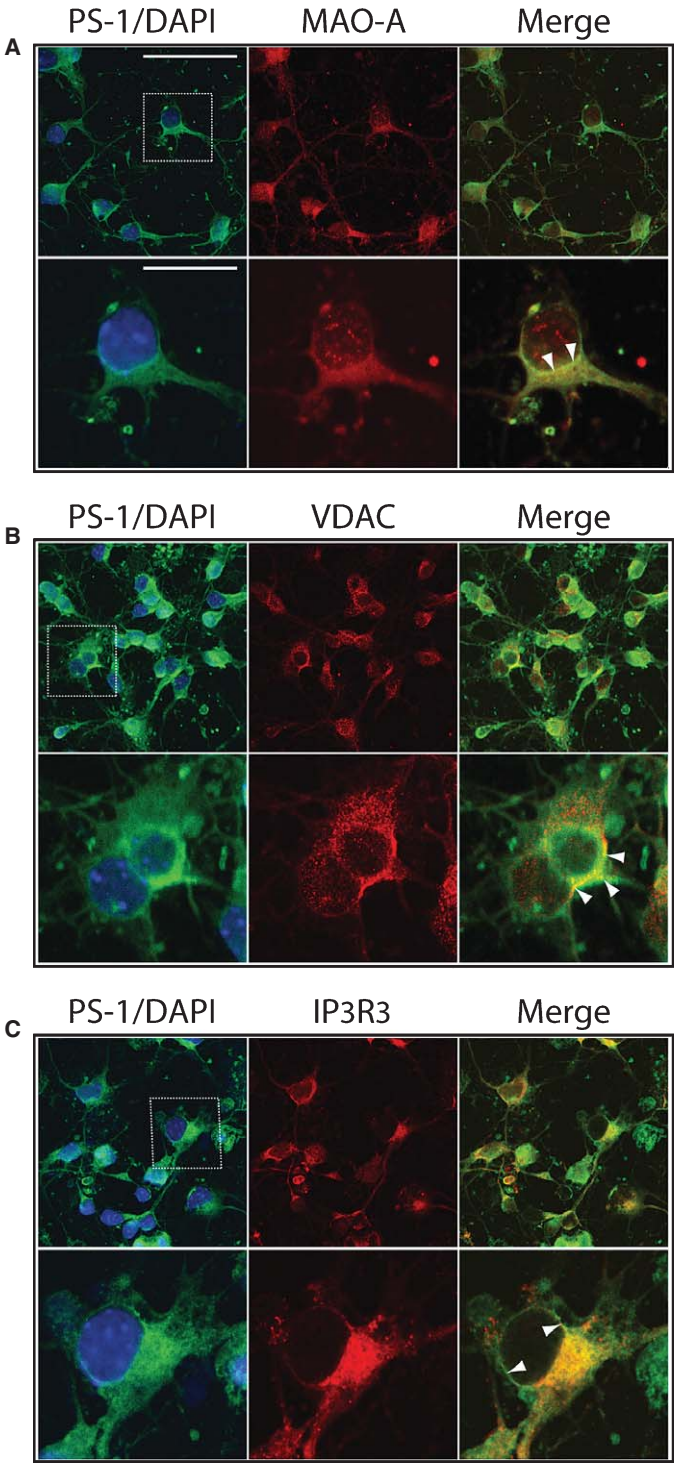

Fig. 7. PS-1 is detected in subcellular regions identified by mitochondrial markers in cortical neurons. Primary cortical neurons (DIV 10) were processed for PS-1 (green in all cases) and the nucleus was stained with DAPI. Cultures were also processed for (A) MAO-A, (B) VDAC, the mitochondrial voltage-dependent anion channel, or (C) IP3R3, a marker for the mitochondrial-associated membrane (MAM) of the ER. In each case a cell in the respective top panel (boxed) was examined at higher magnification. Although PS-1 and the various markers have distinct distributions throughout the cell/organelles, there is also very clear evidence (in the merged image, right panels) of areas of overlap (yellow, selected sites are indicated by arrowheads). The association of PS-1 with the IP3R3/MAM-immunoreactive subcellular compartment is particularly clear.

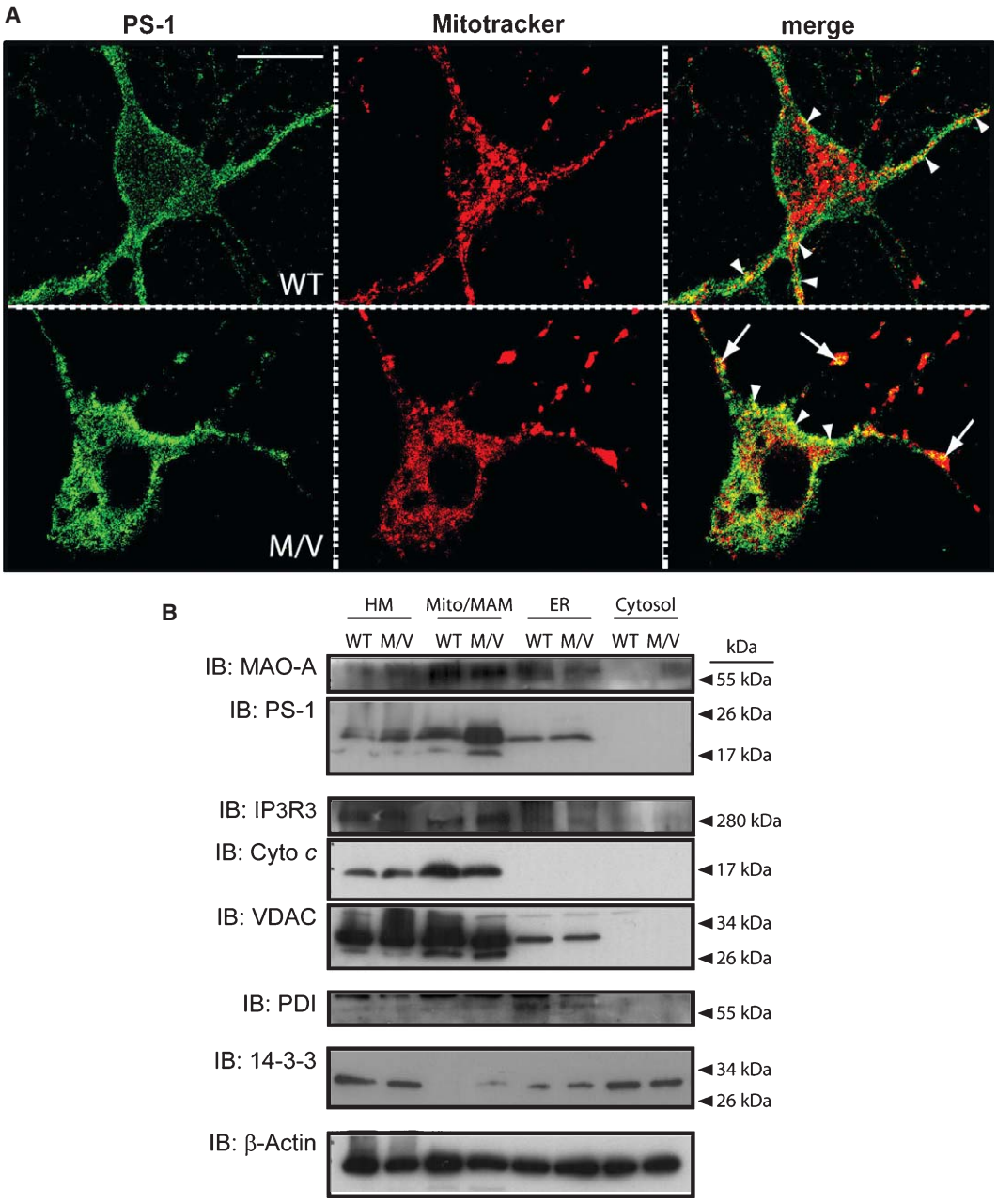

Fig. 8. The PS-1(M146V) protein associates preferentially with the mitochondrial fraction. A) WT and PS-1(M146V) (M/V) primary neurons (DIV 10) were processed for PS-1 (green) and a mitochondrial stain (Mitotracker®, red). The association of PS-1 with the mitochondria in the WT cell is evident in both the cell soma and processes ('yellow' in the merged image; arrowheads). In the M/V cell, the overlap in the soma is more extensive and the two signals tend to accumulate at regular intervals along dystrophic processes (arrows). B) Subcellular fractionation of fresh cortical samples from 6-month old WT and M/V mice were resolved for Western blot and probed for MAO-A (~59 kDa), PS-1 (CTF; ~20 kDa), IP3R3 (~320 kDa: a marker for the MAM), cytochrome *c* (~15 kDa; a marker for the mitochondria), VDAC (~31 kDa; a marker for the mitochondria), PDI (~60 kDa: a marker for the ER), 14-3-3 (~33 kDa: a marker for the cytosol). A strong PS-1(M146V) signal co-segregates with MAO-A in the mitochondrial/MAM fraction. A modest MAO-A signal is detected in the ER-enriched fraction. HM: heavy membrane fraction (cell debris and nuclei); MAM: mitochondria-associated membrane of the ER (*technical note*: the MAM co-segregates with the mitochondrial fraction during differential centrifugation); kDa: molecular weight markers.

blot revealed that PS-1 also segregated with the mitochondrial/MAM fraction (Figs. 7 and 8), thus confirming previous reports [34, 35]. Interestingly, there was a stronger PS-1 immunoreactivity in the PS-1(M146V) mitochondrial/MAM fraction versus the WT mitochondrial/MAM fraction (Figs. 7 and 8). Fractionation was confirmed using specific markers, e.g., VADC and cytochrome *c* co-segregated with the mitochondria/MAM fraction, PDI segregated with the ER-enriched fraction and the 14-3-3 protein segregated primarily with the cytosolic fraction (Fig. 8). Note that the mitochondria and MAM co-fractionated using this centrifugation protocol.

These data (Figs. 6–8) continue to support the possibility that the influence of PS-1(M146V) on cortical MAO-A function results from a physical interaction between these two proteins.

The co-immunoprecipitation of PS-1 and MAO-A proteins from tissues and from N2a extracts confirms a physical interaction between the two proteins

We were able to co-immunoprecipitate endogenous MAO-A with both PS-1 WT and the PS-1(M146V) knock-in variant (Fig. 9A). Although the signal was weak, it should be borne in mind that this represents the average signal across all cell types in the cortex (not all of which might similarly co-express

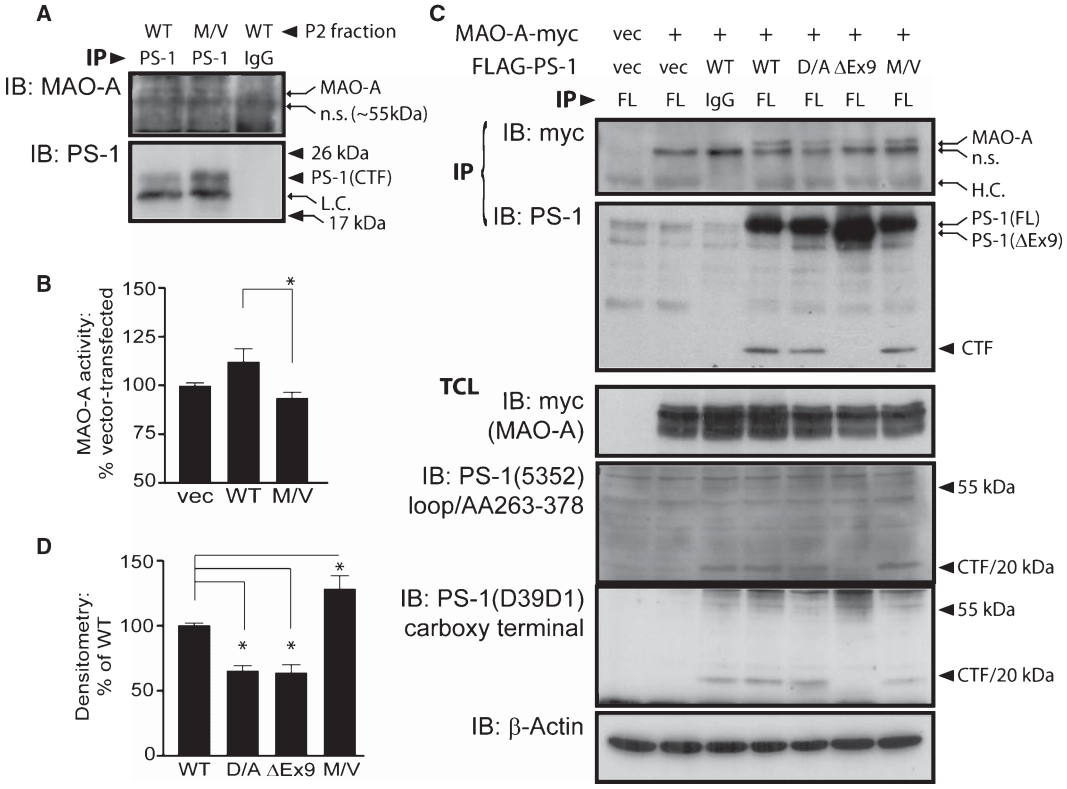

Fig. 9. PS-1 proteins interact with MAO-A *in vitro*. A) Wildtype (WT) and PS-1(M146V) (M/V) mouse cortical mitochondrial (P2) fractions were immunoprecipitated (IP) for PS-1 and resolved proteins were probed for MAO-A and PS-1 (CTF: C-terminal fragment; L.C. light chain of the immunoprecipitating antibody; n.s.: non-specific). B) N2a (neuroblastoma) cultures co-expressing either FLAG-PS-1 WT or FLAG-PS-1(M146V) (M/V) with MAO-A-myc were tested for MAO-A catalytic activity. $*p < 0.05$ between indicated groups ($n = 5$-6, mean ± SEM). C) FLAG-tagged PS-1 variants were co-expressed with myc-tagged MAO-A in N2a cells. Anti-FLAG (FL) or normal (control) mouse IgG immunoprecipitates were probed for myc (e.g., MAO-A-myc) (n.s.: non-specific band; H.C.: heavy chain of the immunoprecipitating anti-FLAG antibody). Parallel immunoprecipitates were probed for PS-1. Note the increased mobility of the ΔEx9 splice site variant (versus FL: full length) and the lack of a C-terminal fragment (CTF) in the same lane. Total cell lysates (TCL) were probed for MAO-A-myc as well as FLAG-PS-1 expression [e.g., by the presence of the CTF (~20 kDa) and the lack thereof in the PS-1(ΔEx9) lysates; note that these band patterns were confirmed using two separate anti-PS-1 antibodies]. D) Densitometric analysis of the co-immunoprecipitation of MAO-A-myc with the PS-1 variants indicated in (C) are expressed as a percentage of the co-immunoprecipitation of MAO-A with WT PS-1. $*p < 0.05$ between indicated groups ($n = 3$–4, mean ± SEM). vec: transfected with empty (FLAG or myc) vector; D/A: PS-1(D257A); ΔEx9: PS-1(ΔEx9); M/V: PS-1(M146V).

PS-1 and MAO-A at the same levels). We chose to explore this further using a model in which both proteins could be overexpressed. N2a cells are functionally deficient in MAO-A and, thus, are optimal for studying aspects of overexpressed MAO-A [62]. We co-expressed FLAG-tagged PS-1 variants with myc-tagged MAO-A and determined that the overexpression of PS-1(M146V) inhibited MAO-A activity (cf., activity in cultures overexpressing PS-1 WT) [$F_{(2,16)} = 5.638$, $p = 0.0160$] (Fig. 9B). In parallel cultures, resolved anti-FLAG immunoprecipitates were probed for MAO-A and confirmed the interaction between PS-1 proteins and MAO-A (Fig. 9C). We included two other PS-1 variants that are known to alter PS-1/γ-secretase-mediated interactions. The deletion of exon 9 abolished proteolytic processing of PS-1, as confirmed by the expected loss [69] of the C-terminal fragment (detected using two anti-PS-1 antibodies targeting distinct epitopes: Fig. 9C). The diminished co-immunoprecipitation between PS-1 (ΔEx9) and MAO-A proteins indicates that the PS-1 loop region is required for the interaction between PS-1 and MAO-A. We also examined the interaction of MAO-A with the PS-1(D257A) active site variant. While this substitution has been shown to block PS-1 endoproteolysis [70], this was not the case in N2a cells (Fig. 9C), thus also corroborating similar observations in other cell lines [71, 72]. The D257A substitution is known to interfere with PS-1/γ-secretase substrate binding and processing [72, 73], and the diminished interaction between this variant and MAO-A (Fig. 9C) provides additional evidence that MAO-A is a novel binding partner for PS-1. Densitometry (Fig. 9D) confirmed the differences in interactions between PS-1 variants and the MAO-A protein [$F_{(3,13)} = 25.11$, $p < 0.0001$].

DISCUSSION

Some of the earliest lesions in AD brain occur in regions highly immunoreactive for MAO-A, such as the nucleus basalis of Meynert and the locus coeruleus [14, 23, 74]. Altered biogenic neurotransmitter metabolism and receptor density in several models of AD are believed to be epiphenomena of the amyloid burden incurred by a given transgene [30, 31]. Although one could speculate as to the role of MAO in this context, our data are the first to provide evidence for the *in vivo* dysregulation of MAO catalytic function in an AD-related background, i.e., in the PS-1(M146V) knock-in mouse.

The PS-1 protein physically associates with the MAO-A protein

The expression of the PS-1(M146V) protein is tightly controlled and is known to simply displace its endogenous counterpart [75, 76]. While its overexpression *in vivo* may not be that evident, its influence on cortical MAO-A function is undeniable. The increased MAO-A activity in PS-1(M146V) cortical homogenates induced by the PS-1/γ-secretase substrate-competitive inhibitor, DAPT, supports our conclusion (based on neurochemical, microscopy and subcellular fractionation studies) of a direct inhibition of MAO-A function by PS-1(M146V), and furthermore corroborates the reported functional differences between PS-1 WT and variants [77]. These differences could be reflecting mutation-dependent conformational changes in PS-1 that are known to affect interactions with binding partners and substrates [70].

The fact that MAO-A co-immunoprecipitates better with PS-1(M146V) is not surprising given the preferential segregation of PS-1(M146V) with the mitochondrial/MAM fraction (present study) and given the tighter binding capacity of PS-1 mutants towards other targets, for example the p70CLIP protein [78]. The co-immunoprecipitation of PS-1 and MAO-A is clearly reduced in cultures expressing the PS-1(D257A) active site variant or the PS-1(ΔEx9) splice site variant, both of which are well known to disrupt PS-1/γ-secretase substrate binding. We have recently confirmed the physical interaction between ectopic PS-1 and MAO-A proteins in other cell lines, i.e., the HT-22 mouse hippocampal line and the HEK293 human embryonic kidney line [79]. Although MAO-A does not conform to the type I transmembrane protein structure that is typical of PS-1/γ-secretase targets [80], this would not necessarily preclude its potential for binding to the PS-1/γ-secretase complex, but would simply preclude its access to the active site [81]. At this juncture, one could certainly question why MAO-A has not yet been identified as a binding partner for PS-1, given the wide range of reported substrates [82]. Our hypothesis would posit that the interaction of MAO-A with PS-1 requires the intact γ-secretase complex and would not be identified in screens for [single] protein-protein interactions, such as with the yeast two-hybrid system. In support of this, the most studied substrate for the PS-1/γ-secretase complex, AβPP, is not identified when PS-1 is used as 'bait' in a yeast two-hybrid system [83, 84].

PS-1(M146V) affects MAO-A-sensitive monoaminergic tone

The MAO-A-dependent changes in monoaminergic function in 6 month-old PS-1(M146V) mice, when AD-related neuropathology is clearly absent [85], implicate a novel Aβ/AβPP-independent effect of PS-1/γ-secretase in AD-related neuropsychiatric sequelae. Our data reveal an induction of MAO-A protein in the PS-1(M146V) mouse cortex, yet MAO-A activity in corresponding homogenates is not similarly increased. This, in combination with the results of our neurochemical analyses, suggests an inhibition of MAO-A by the PS-1(M146V) variant. Such an influence of a PS-1 variant on monoaminergic tone in AD subjects could explain, in part, why 5-HT terminal fields and neurons of the raphé nuclei (contain 5-HT cell bodies) are rife with neurofibrillary tangles [86–88]. Our ongoing work suggests subtle differences in MAO-A function in PS-1(M146V) mouse cerebellum. Region-specific effects of AD-related PS-1 variants are not unique as carriers of the PS-1(ΔEx9) variant present with different plaque conformations and Aβ peptide constituents in the frontal cortex versus the cerebellum [89], whereas a variety of other mutations in PS-1 affect the regional expression of the PS-1 protein and exert distinct effects on Aβ burden [90].

Aside from its role in AD-related neuropathology [91], PS-1 also mediates normal development of the cerebral cortex [92, 93]. The patchy distribution of Nissl substance and disrupted laminar boundaries in the PS-1(M146V) mouse cortex (present study) corroborate reports of disrupted cortical lamination in both prenatal PS-1-null mice [94] and postnatal PS-1 conditional knockout mice [93]. Furthermore, axonal transport is affected in the PS-1(M146V) mouse [95], which could certainly explain the dystrophic processes and mitochondrial aggregation we observe in primary PS-1(M146V) neurons as well as the accumulation of MAO-A signal within the neuropil of the PS-1(M146V) mouse cortex and the associated architectural changes. Serotonergic fibers are among the earliest to reach the developing cerebral cortex [96]. The permanent cytoarchitectural alterations observed in the somatosensory cortex of MAO-A-knockout mice [97] or as a consequence of MAO-A inhibitor-mediated hyperserotonergic (but not noradrenergic) tone during the first week of life in normal mice [98] support the developmental changes and the diminished proliferation of neural stem cells observed recently in MAO-A/B knockout mice [99]. We are currently examining the role of MAO-A in cortical laminar disorganization in PS-1(M146V) mice. *A priori*, if PS-1(M146V) is inhibiting MAO-A, as our data indicate, then a role for MAO-A in this phenomenon is certainly feasible. By extension, this would strongly suggest that certain cases of AD, particularly those with an early onset/genetic progression, might have a *developmental* etiology rather than being strictly dependent on premature cellular senescence and enhanced Aβ burden as championed by the current paradigm. The clinical and empirical evidence in support of the Aβ hypothesis of AD has come under scrutiny lately [100, 101] and alternate hypotheses clearly need to be explored.

The PS-1(M146V) knock-in mouse exhibits MAO-A-sensitive non-cognitive behaviors

Cognitive dysfunction and memory loss are characteristics of the later stages of clinical AD. Yet earlier stages of AD are also associated with several non-cognitive, neuropsychiatric symptoms including depression, irritability, aggressive outbursts, and delusions [4]. It is well known that these disorders reflect region-specific noradrenergic and serotonergic insults and, as such, it is not surprising that monoaminergic metabolism is altered in the PS-1(M146V) mouse. The fact that noradrenergic changes were greater than serotonergic changes following acute inhibition of MAO-A with CLG is not unexpected [102, 103], as MAO-A is expressed primarily in catecholaminergic, i.e., noradrenergic, neurons [this is designed to eliminate foreign amines, including serotonin, that could diffuse from neighboring synapses and potentially disrupt synaptic noradrenergic vesicles] [104]. Exacerbated changes in noradrenergic and serotonergic metabolism following acute MAO-A inhibition would certainly contribute to the changes we observe in the swimming (non-cognitive) behavior of the PS-1(M146V) mice.

Could our observed MAO-A-sensitive effects on non-cognitive behavior and monoaminergic metabolism explain the increased incidence of depression associated with earlier pre-dementia stages of AD [74, 105–108]? This is a reasonable hypothesis given that depression and psychiatric symptoms precede the dementia associated with the PS-1(L173F) substitution [109], whereas mood symptoms and depression are evident at the onset of disease associated with the PS-1(L392P) [110] and PS-1(L250S) [111] substitutions. Furthermore, the incidence of depression is increased in pre-demented carriers of the AD-related A431E, L235V and E280A substitutions in the *PSEN1* gene [39, 112]. We have demonstrated [79] that the A431E and L235V

PS-1 variants can induce MAO-A activity (which would be expected in clinical depression; [113]). We have also observed differences *in vitro* in MAO-A activity in response to two very aggressive AD-related PS-1 variants [61], namely PS-1(Y115H) [no effect on MAO-A activity] and PS-1(ΔEx9) (increases MAO-A activity by ∼20%) [79]. Although the latter observation would certainly argue for an increased incidence of clinical depression in carriers of the PS-1(ΔEx9) variant, this has never been documented. Also, we would not expect the PS-1(M146V) variant to support a prodromal depressive phenotype as PS-1(M146V) *inhibits* MAO-A. Differences in the effects of PS-1 variants on cellular mechanisms and phenotypes are well documented and a direct role for some variants in depression is certainly feasible. It is expected that multiple mechanisms of actions would be involved, including mechanisms dependent on MAO-A dysfunction.

The PS-1(M146V) protein alters MAO-A inhibitor potency

AD-related mutations in the PS-1 protein are known to exert conformational changes [70]. Perhaps by virtue of a direct interaction between PS-1(M146V) and MAO-A, a concomitant change in the structure of MAO-A could explain the increased potency of CLG we observed in the PS-1(M146V) mouse cortical samples. A conformational change in the MAO-A protein could certainly alter the accessibility of CLG to its binding site, which could promote an apparent change in the Hill slope. Such an increase in cooperativity would suggest partially interconvertible states of a single CLG binding site. Yet, PS-1-dependent post-translational mechanisms based on activation of distinct signaling cascades [114], several of which have been found to influence MAO-A function [62], could certainly also be involved.

Future considerations

An understanding of endogenous mechanisms for the regulation of MAO is important for understanding its role in both normal physiology and pathology. We now demonstrate that MAO-A function can be altered significantly by an AD-related PS-1 protein. Furthermore, we identify MAO-A as a novel binding partner for PS-1. Our data also suggest that pharmacological MAO-A inhibition could exert non-cognitive effects in certain patients predisposed to AD (could this be extrapolated to other monoamine-altering therapeutics?, see [115]). This could potentially extend to patients with a form of AD that is not necessarily predicated on a mutation in the *PSEN-1* gene, but is associated with other risk factors, e.g., the APOE4 allele in combination with polymorphisms in both the 5-HT transporter and MAO-A [10]. Our data provide for a unique function for PS-1/γ-secretase and further characterization, both *in vivo* and *in vitro*, is clearly required. This endogenous means of regulating MAO-A function could have serious biological implications and needs to be duly considered when interpreting experimental and clinical PS-1- and/or MAO-A-sensitive pathologies, particularly those with a neurochemical overlap and such social impact as depression and AD.

ACKNOWLEDGMENTS

Part of this work was presented at the 2010 Amine Oxidase Workshop (Edmonton, Alberta, Canada). We thank Tuo Zhao, David Woloschuk, Gail Rauw and Tanya Lehmann for technical support and Dr. Scot Leary for advice with the subcellular fractionation. This work was funded by departmental research awards, e.g., Alfred E. Molstad Trust Awards and Aruna and Kripa Thakur Awards (to GGG & XC), by a College of Graduate Studies Dean's Scholarship and a Canadian Institutes of Health Research (CIHR) Master's Scholarship (both to GGG), and by a CIHR-Saskatchewan Health Research Foundation (SHRF) Operating Grant (DDM). GBB holds a University of Alberta Distinguished University Professor Award. DDM holds the Saskatchewan Research Chair in *Alzheimer's Disease and Related Dementias* funded jointly by the Alzheimer Society of Saskatchewan and the SHRF.

Authors' disclosures available online (http://www.j-alz.com/disclosures/view.php?id=1003).

REFERENCES

[1] Coppen A (1967) The biochemistry of affective disorders. *Br J Psychiatry* **113**, 1237-1264.
[2] Schildkraut JJ (1965) The catecholamine hypothesis of affective disorders: A review of supporting evidence. *Am J Psychiatry* **122**, 509-522.
[3] Naoi M, Maruyama W (2010) Monoamine oxidase inhibitors as neuroprotective agents in age-dependent neurodegenerative disorders. *Curr Pharm Des* **16**, 2799-2817.
[4] Ritchie K, Lovestone S (2002) The dementias. *Lancet* **360**, 1759-1766.
[5] Caraci F, Copani A, Nicoletti F, Drago F (2010) Depression and Alzheimer's disease: Neurobiological links and

common pharmacological targets. *Eur J Pharmacol* **626**, 64-71.

[6] Geerlings MI, den Heijer T, Koudstaal PJ, Hofman A, Breteler MM (2008) History of depression, depressive symptoms, and medial temporal lobe atrophy and the risk of Alzheimer disease. *Neurology* **70**, 1258-1264.

[7] Wuwongse S, Chang RC, Law AC (2010) The putative neurodegenerative links between depression and Alzheimer's disease. *Prog Neurobiol* **91**, 362-375.

[8] Kessing LV, Andersen PK (2004) Does the risk of developing dementia increase with the number of episodes in patients with depressive disorder and in patients with bipolar disorder? *J Neurol Neurosurg Psychiatry* **75**, 1662-1666.

[9] Du L, Faludi G, Palkovits M, Sotonyi P, Bakish D, Hrdina PD (2002) High activity-related allele of MAO-A gene associated with depressed suicide in males. *Neuroreport* **13**, 1195-1198.

[10] Nishimura AL, Guindalini C, Oliveira JR, Nitrini R, Bahia VS, de Brito-Marques PR, Otto PA, Zatz M (2005) Monoamine oxidase a polymorphism in Brazilian patients: Risk factor for late-onset Alzheimer's disease? *J Mol Neurosci* **27**, 213-217.

[11] Takehashi M, Tanaka S, Masliah E, Ueda K (2002) Association of monoamine oxidase A gene polymorphism with Alzheimer's disease and Lewy body variant. *Neurosci Lett* **327**, 79-82.

[12] Wu YH, Fischer DF, Swaab DF (2007) A promoter polymorphism in the monoamine oxidase A gene is associated with the pineal MAOA activity in Alzheimer's disease patients. *Brain Res* **1167**, 13-19.

[13] Burke WJ, Li SW, Chung HD, Ruggiero DA, Kristal BS, Johnson EM, Lampe P, Kumar VB, Franko M, Williams EA, Zahm DS (2004) Neurotoxicity of MAO metabolites of catecholamine neurotransmitters: Role in neurodegenerative diseases. *Neurotoxicology* **25**, 101-115.

[14] Grudzien A, Shaw P, Weintraub S, Bigio E, Mash DC, Mesulam MM (2007) Locus coeruleus neurofibrillary degeneration in aging, mild cognitive impairment and early Alzheimer's disease. *Neurobiol Aging* **28**, 327-335.

[15] Marcyniuk B, Mann DM, Yates PO (1986) Loss of nerve cells from locus coeruleus in Alzheimer's disease is topographically arranged. *Neurosci Lett* **64**, 247-252.

[16] Parvizi J, Van Hoesen GW, Damasio A (2001) The selective vulnerability of brainstem nuclei to Alzheimer's disease. *Ann Neurol* **49**, 53-66.

[17] Rub U, Del Tredici K, Schultz C, Thal DR, Braak E, Braak H (2000) The evolution of Alzheimer's disease-related cytoskeletal pathology in the human raphe nuclei. *Neuropathol Appl Neurobiol* **26**, 553-567.

[18] Zweig RM, Ross CA, Hedreen JC, Steele C, Cardillo JE, Whitehouse PJ, Folstein MF, Price DL (1988) The neuropathology of aminergic nuclei in Alzheimer's disease. *Ann Neurol* **24**, 233-242.

[19] Kennedy BP, Ziegler MG, Alford M, Hansen LA, Thal LJ, Masliah E (2003) Early and persistent alterations in prefrontal cortex MAO A and B in Alzheimer's disease. *J Neural Transm* **110**, 789-801.

[20] Emilsson L, Saetre P, Balciuniene J, Castensson A, Cairns N, Jazin EE (2002) Increased monoamine oxidase messenger RNA expression levels in frontal cortex of Alzheimer's disease patients. *Neurosci Lett* **326**, 56-60.

[21] Sparks DL, Woeltz VM, Markesbery WR (1991) Alterations in brain monoamine oxidase activity in aging, Alzheimer's disease, and Pick's disease. *Arch Neurol* **48**, 718-721.

[22] Sherif F, Gottfries CG, Alafuzoff I, Oreland L (1992) Brain gamma-aminobutyrate aminotransferase (GABA-T) and monoamine oxidase (MAO) in patients with Alzheimer's disease. *J Neural Transm Park Dis Dement Sect* **4**, 227-240.

[23] Chan-Palay V, Hochli M, Savaskan E, Hungerecker G (1993) Calbindin D-28k and monoamine oxidase A immunoreactive neurons in the nucleus basalis of meynert in senile dementia of the Alzheimer type and Parkinson's disease. *Dementia* **4**, 1-15.

[24] Burke WJ, Li SW, Schmitt CA, Xia P, Chung HD, Gillespie KN (1999) Accumulation of 3,4-dihydroxyphenylglycolaldehyde, the neurotoxic monoamine oxidase A metabolite of norepinephrine, in locus ceruleus cell bodies in Alzheimer's disease: Mechanism of neuron death. *Brain Res* **816**, 633-637.

[25] Nazarali AJ, Reynolds GP (1992) Monoamine neurotransmitters and their metabolites in brain regions in Alzheimer's disease: A postmortem study. *Cell Mol Neurobiol* **12**, 581-587.

[26] Gundlah C, Lu NZ, Bethea CL (2002) Ovarian steroid regulation of monoamine oxidase-A and -B mRNAs in the macaque dorsal raphe and hypothalamic nuclei. *Psychopharmacology (Berl)* **160**, 271-282.

[27] Holschneider DP, Kumazawa T, Chen K, Shih JC (1998) Tissue-specific effects of estrogen on monoamine oxidase A and B in the rat. *Life Sci* **63**, 155-160.

[28] Ou XM, Chen K, Shih JC (2006) Monoamine oxidase A and repressor R1 are involved in apoptotic signaling pathway. *Proc Natl Acad Sci U S A* **103**, 10923-10928.

[29] Fitzgerald JC, Ufer C, Billett EE (2007) A link between monoamine oxidase-A and apoptosis in serum deprived human SH-SY5Y neuroblastoma cells. *J Neural Transm* **114**, 807-810.

[30] Liu Y, Yoo MJ, Savonenko A, Stirling W, Price DL, Borchelt DR, Mamounas L, Lyons WE, Blue ME, Lee MK (2008) Amyloid pathology is associated with progressive monoaminergic neurodegeneration in a transgenic mouse model of Alzheimer's disease. *J Neurosci* **28**, 13805-13814.

[31] Szapacs ME, Numis AL, Andrews AM (2004) Late onset loss of hippocampal 5-HT and NE is accompanied by increases in BDNF protein expression in mice co-expressing mutant APP and PS1. *Neurobiol Dis* **16**, 572-580.

[32] Roychaudhuri R, Yang M, Hoshi MM, Teplow DB (2009) Amyloid beta-protein assembly and Alzheimer disease. *J Biol Chem* **284**, 4749-4753.

[33] Yankner BA, Lu T (2009) Amyloid beta-protein toxicity and the pathogenesis of Alzheimer disease. *J Biol Chem* **284**, 4755-4759.

[34] Ankarcrona M, Hultenby K (2002) Presenilin-1 is located in rat mitochondria. *Biochem Biophys Res Commun* **295**, 766-770.

[35] Hansson CA, Frykman S, Farmery MR, Tjernberg LO, Nilsberth C, Pursglove SE, Ito A, Winblad B, Cowburn RF, Thyberg J, Ankarcrona M (2004) Nicastrin, presenilin, APH-1, and PEN-2 form active gamma-secretase complexes in mitochondria. *J Biol Chem* **279**, 51654-51660.

[36] De Strooper B, Beullens M, Contreras B, Levesque L, Craessaerts K, Cordell B, Moechars D, Bollen M, Fraser P, George-Hyslop PS, Van Leuven F (1997) Phosphorylation, subcellular localization, and membrane orientation of the Alzheimer's disease-associated presenilins. *J Biol Chem* **272**, 3590-3598.

[37] Area-Gomez E, de Groof AJ, Boldogh I, Bird TD, Gibson GE, Koehler CM, Yu WH, Duff KE, Yaffe MP, Pon LA, Schon EA (2009) Presenilins are enriched in endoplasmic

reticulum membranes associated with mitochondria. *Am J Pathol* **175**, 1810-1816.
[38] Wiedemann N, Meisinger C, Pfanner N (2009) Cell biology. Connecting organelles. *Science* **325**, 403-404.
[39] Ringman JM, Diaz-Olavarrieta C, Rodriguez Y, Chavez M, Paz F, Murrell J, Macias MA, Hill M, Kawas C (2004) Female preclinical presenilin-1 mutation carriers unaware of their genetic status have higher levels of depression than their non-mutation carrying kin. *J Neurol Neurosurg Psychiatry* **75**, 500-502.
[40] Comery TA, Martone RL, Aschmies S, Atchison KP, Diamantidis G, Gong X, Zhou H, Kreft AF, Pangalos MN, Sonnenberg-Reines J, Jacobsen JS, Marquis KL (2005) Acute gamma-secretase inhibition improves contextual fear conditioning in the Tg2576 mouse model of Alzheimer's disease. *J Neurosci* **25**, 8898-8902.
[41] Pakaski M, Bjelik A, Hugyecz M, Kasa P, Janka Z, Kalman J (2005) Imipramine and citalopram facilitate amyloid precursor protein secretion *in vitro*. *Neurochem Int* **47**, 190-195.
[42] Ash ES, Alavijeh MS, Palmer AM, Mitchelmore C, Howlett DR, Francis PT, Broadstock M, Richardson JC (2010) Neurochemical changes in a double transgenic mouse model of Alzheimer's disease fed a pro-oxidant diet. *Neurochem Int* **57**, 504-511.
[43] Pugh PL, Richardson JC, Bate ST, Upton N, Sunter D (2007) Non-cognitive behaviours in an APP/PS1 transgenic model of Alzheimer's disease. *Behav Brain Res* **178**, 18-28.
[44] Zhu X, Flint Beal M, Wang W, Perry G, Smith MA, (Eds) (2010) Mitochondria and neurodegenerative diseases. *J Alzheimers Dis* **20**(Suppl 2), 253-643.
[45] Frisoni GB, Prestia A, Rasser PE, Bonetti M, Thompson PM (2009) In vivo mapping of incremental cortical atrophy from incipient to overt Alzheimer's disease. *J Neurol* **256**, 916-924.
[46] Larner AJ, Ray PS, Doran M (2007) The R269H mutation in presenilin-1 presenting as late-onset autosomal dominant Alzheimer's disease. *J Neurol Sci* **252**, 173-176.
[47] Guo Q, Fu W, Sopher BL, Miller MW, Ware CB, Martin GM, Mattson MP (1999) Increased vulnerability of hippocampal neurons to excitotoxic necrosis in presenilin-1 mutant knock-in mice. *Nat Med* **5**, 101-106.
[48] Auffret A, Gautheron V, Mattson MP, Mariani J, Rovira C (2010) Progressive age-related impairment of the late long-term potentiation in Alzheimer's disease presenilin-1 mutant knock-in mice. *J Alzheimers Dis* **19**, 1021-1033.
[49] Odero GL, Oikawa K, Glazner KA, Schapansky J, Grossman D, Thiessen JD, Motnenko A, Ge N, Martin M, Glazner GW, Albensi BC (2010) Evidence for the involvement of calbindin D28k in the presenilin 1 model of Alzheimer's disease. *Neuroscience* **169**, 532-543.
[50] Cao X, Rui L, Pennington PR, Chlan-Fourney J, Jiang Z, Wei Z, Li XM, Edmondson DE, Mousseau DD (2009) Serine 209 resides within a putative p38(MAPK) consensus motif and regulates monoamine oxidase-A activity. *J Neurochem* **111**, 101-110.
[51] Brown GD, Nazarali AJ (2010) Matrix metalloproteinase-25 has a functional role in mouse secondary palate development and is a downstream target of TGF-beta3. *BMC Dev Bio* **10**, 93.
[52] Cao X, Wei Z, Gabriel GG, Li X, Mousseau DD (2007) Calcium-sensitive regulation of monoamine oxidase-A contributes to the production of peroxyradicals in hippocampal cultures: Implications for Alzheimer disease-related pathology. *BMC Neurosci* **8**, 73.
[53] Wei Z, Chigurupati S, Arumugam TV, Jo DG, Li H, Chan SL (2011) Notch activation enhances the microglia-mediated inflammatory response associated with focal cerebral ischemia. *Stroke* **42**, 2589-2594.
[54] Wieckowski MR, Giorgi C, Lebiedzinska M, Duszynski J, Pinton P (2009) Isolation of mitochondria-associated membranes and mitochondria from animal tissues and cells. *Nat Protoc* **4**, 1582-1590.
[55] Porsolt RD, Bertin A, Jalfre M (1977) Behavioral despair in mice: A primary screening test for antidepressants. *Arch Int Pharmacodyn Ther* **229**, 327-336.
[56] Potter WZ, Murphy DL, Wehr TA, Linnoila M, Goodwin FK (1982) Clorgyline. A new treatment for patients with refractory rapid-cycling disorder. *Arch Gen Psychiatry* **39**, 505-510.
[57] Lipper S, Murphy DL, Slater S, Buchsbaum MS (1979) Comparative behavioral effects of clorgyline and pargyline in man: A preliminary evaluation. *Psychopharmacology (Berl)* **62**, 123-128.
[58] Nielsen DM, Carey GJ, Gold LH (2004) Antidepressant-like activity of corticotropin-releasing factor type-1 receptor antagonists in mice. *Eur J Pharmacol* **499**, 135-146.
[59] Kitanaka N, Kitanaka J, Takemura M (2005) Inhibition of methamphetamine-induced hyperlocomotion in mice by clorgyline, a monoamine oxidase-a inhibitor, through alteration of the 5-hydroxytriptamine turnover in the striatum. *Neuroscience* **130**, 295-308.
[60] Mousseau DD, Greenshaw AJ (1989) Chronic effects of clomipramine and clorgyline on regional levels of brain amines and acid metabolites in rats. *J Neural Transm* **75**, 73-79.
[61] Hebert SS, Godin C, Tomiyama T, Mori H, Levesque G (2003) Dimerization of presenilin-1 *in vivo*: Suggestion of novel regulatory mechanisms leading to higher order complexes. *Biochem Biophys Res Commun* **301**, 119-126.
[62] Cao X, Li XM, Mousseau DD (2009) Calcium alters monoamine oxidase-A parameters in human cerebellar and rat glial C6 cell extracts: Possible influence by distinct signalling pathways. *Life Sci* **85**, 262-268.
[63] Fitzgerald JC, Ufer C, De Girolamo LA, Kuhn H, Billett EE (2007) Monoamine oxidase-A modulates apoptotic cell death induced by staurosporine in human neuroblastoma cells. *J Neurochem* **103**, 2189-2199.
[64] Fowler JS, Alia-Klein N, Kriplani A, Logan J, Williams B, Zhu W, Craig IW, Telang F, Goldstein R, Volkow ND, Vaska P, Wang GJ (2007) Evidence that brain MAO A activity does not correspond to MAO A genotype in healthy male subjects. *Biol Psychiatry* **62**, 355-358.
[65] Petit-Demouliere B, Chenu F, Bourin M (2005) Forced swimming test in mice: A review of antidepressant activity. *Psychopharmacology (Berl)* **177**, 245-255.
[66] Morohashi Y, Kan T, Tominari Y, Fuwa H, Okamura Y, Watanabe N, Sato C, Natsugari H, Fukuyama T, Iwatsubo T, Tomita T (2006) C-terminal fragment of presenilin is the molecular target of a dipeptidic gamma-secretase-specific inhibitor DAPT (N-[N-(3,5-difluorophenacetyl)-L-alanyl]-S-phenylglycine t-butyl ester). *J Biol Chem* **281**, 14670-14676.
[67] Yang T, Arslanova D, Gu Y, Augelli-Szafran C, Xia W (2008) Quantification of gamma-secretase modulation differentiates inhibitor compound selectivity between two substrates Notch and amyloid precursor protein. *Mol Brain* **1**, 15.
[68] Hayashi T, Rizzuto R, Hajnoczky G, Su TP (2009) MAM: More than just a housekeeper. *Trends Cell Biol* **19**, 81-88.

[69] Thinakaran G, Borchelt DR, Lee MK, Slunt HH, Spitzer L, Kim G, Ratovitsky T, Davenport F, Nordstedt C, Seeger M, Hardy J, Levey AI, Gandy SE, Jenkins NA, Copeland NG, Price DL, Sisodia SS (1996) Endoproteolysis of presenilin 1 and accumulation of processed derivatives *in vivo*. *Neuron* **17**, 181-190.

[70] Berezovska O, Lleo A, Herl LD, Frosch MP, Stern EA, Bacskai BJ, Hyman BT (2005) Familial Alzheimer's disease presenilin 1 mutations cause alterations in the conformation of presenilin and interactions with amyloid precursor protein. *J Neurosci* **25**, 3009-3017.

[71] Nyabi O, Bentahir M, Horre K, Herreman A, Gottardi-Littell N, Van Broeckhoven C, Merchiers P, Spittaels K, Annaert W, De Strooper B (2003) Presenilins mutated at Asp-257 or Asp-385 restore Pen-2 expression and Nicastrin glycosylation but remain catalytically inactive in the absence of wild type presenilin. *J Biol Chem* **278**, 43430-43436.

[72] Kim H, Ki H, Park HS, Kim K (2005) Presenilin-1 D257A and D385A mutants fail to cleave Notch in their endoproteolyzed forms, but only presenilin-1 D385A mutant can restore its gamma-secretase activity with the compensatory overexpression of normal C-terminal fragment. *J Biol Chem* **280**, 22462-22472.

[73] Wolfe MS, Xia W, Ostaszewski BL, Diehl TS, Kimberly WT, Selkoe DJ (1999) Two transmembrane aspartates in presenilin-1 required for presenilin endoproteolysis and gamma-secretase activity. *Nature* **398**, 513-517.

[74] Chan-Palay V (1992) Depression and senile dementia of the Alzheimer type: A role for moclobemide. *Psychopharmacology (Berl)* **106**(Suppl), S137-S139.

[75] Chan SL, Mayne M, Holden CP, Geiger JD, Mattson MP (2000) Presenilin-1 mutations increase levels of ryanodine receptors and calcium release in PC12 cells and cortical neurons. *J Biol Chem* **275**, 18195-18200.

[76] Kulic L, Walter J, Multhaup G, Teplow DB, Baumeister R, Romig H, Capell A, Steiner H, Haass C (2000) Separation of presenilin function in amyloid beta-peptide generation and endoproteolysis of Notch. *Proc Natl Acad Sci U S A* **97**, 5913-5918.

[77] Shen J, Kelleher RJ, 3rd (2007) The presenilin hypothesis of Alzheimer's disease: Evidence for a loss-of-function pathogenic mechanism. *Proc Natl Acad Sci U S A* **104**, 403-409.

[78] Johnsingh AA, Johnston JM, Merz G, Xu J, Kotula L, Jacobsen JS, Tezapsidis N (2000) Altered binding of mutated presenilin with cytoskeleton-interacting proteins. *FEBS Lett* **465**, 53-58.

[79] Pennington PR, Wei Z, Rui L, Doig JA, Graham B, Kuski K, Gabriel GG, Mousseau DD (2011) Alzheimer disease-related presenilin-1 variants exert distinct effects on monoamine oxidase-A activity *in vitro*. *J Neural Transm* **118**, 987-995.

[80] Steiner H, Fluhrer R, Haass C (2008) Intramembrane proteolysis by gamma-secretase. *J Biol Chem* **283**, 29627-29631.

[81] Wolfe MS (2006) The gamma-secretase complex: Membrane-embedded proteolytic ensemble. *Biochemistry* **45**, 7931-7939.

[82] Vetrivel KS, Zhang YW, Xu H, Thinakaran G (2006) Pathological and physiological functions of presenilins. *Mol Neurodegen* **1**, 4.

[83] Kim SS, Choi YM, Suh YH (1997) Lack of interactions between amyloid precursor protein and hydrophilic domains of presenilin 1 and 2 using the yeast two hybrid system. *J Mol Neurosci* **9**, 49-54.

[84] Hebert SS, Bourdages V, Godin C, Ferland M, Carreau M, Levesque G (2003) Presenilin-1 interacts directly with the beta-site amyloid protein precursor cleaving enzyme (BACE1). *Neurobiol Dis* **13**, 238-245.

[85] van Groen T, Kiliaan AJ, Kadish I (2006) Deposition of mouse amyloid beta in human APP/PS1 double and single AD model transgenic mice. *Neurobiol Dis* **23**, 653-662.

[86] Arai H, Kosaka K, Iizuka R (1984) Changes of biogenic amines and their metabolites in postmortem brains from patients with Alzheimer-type dementia. *J Neurochem* **43**, 388-393.

[87] Curcio CA, Kemper T (1984) Nucleus raphe dorsalis in dementia of the Alzheimer type: Neurofibrillary changes and neuronal packing density. *J Neuropathol Exp Neurol* **43**, 359-368.

[88] Ishii T (1966) Distribution of Alzheimer's neurofibrillary changes in the brain stem and hypothalamus of senile dementia. *Acta Neuropathol* **6**, 181-187.

[89] Mann DM, Takeuchi A, Sato S, Cairns NJ, Lantos PL, Rossor MN, Haltia M, Kalimo H, Iwatsubo T (2001) Cases of Alzheimer's disease due to deletion of exon 9 of the presenilin-1 gene show an unusual but characteristic beta-amyloid pathology known as 'cotton wool' plaques. *Neuropathol Appl Neurobiol* **27**, 189-196.

[90] Verdile G, Gnjec A, Miklossy J, Fonte J, Veurink G, Bates K, Kakulas B, Mehta PD, Milward EA, Tan N, Lareu R, Lim D, Dharmarajan A, Martins RN (2004) Protein markers for Alzheimer disease in the frontal cortex and cerebellum. *Neurology* **63**, 1385-1392.

[91] Price DL, Sisodia SS (1998) Mutant genes in familial Alzheimer's disease and transgenic models. *Annu Rev Neurosci* **21**, 479-505.

[92] Shen J, Bronson RT, Chen DF, Xia W, Selkoe DJ, Tonegawa S (1997) Skeletal and CNS defects in presenilin-1-deficient mice. *Cell* **89**, 629-639.

[93] Wines-Samuelson M, Handler M, Shen J (2005) Role of presenilin-1 in cortical lamination and survival of Cajal-Retzius neurons. *Dev Biol* **277**, 332-346.

[94] Louvi A, Sisodia SS, Grove EA (2004) Presenilin 1 in migration and morphogenesis in the central nervous system. *Development* **131**, 3093-3105.

[95] Pigino G, Morfini G, Pelsman A, Mattson MP, Brady ST, Busciglio J (2003) Alzheimer's presenilin 1 mutations impair kinesin-based axonal transport. *J Neurosci* **23**, 4499-4508.

[96] Dori I, Dinopoulos A, Blue ME, Parnavelas JG (1996) Regional differences in the ontogeny of the serotonergic projection to the cerebral cortex. *Exp Neurol* **138**, 1-14.

[97] Cases O, Seif I, Grimsby J, Gaspar P, Chen K, Pournin S, Muller U, Aguet M, Babinet C, Shih JC et al (1995) Aggressive behavior and altered amounts of brain serotonin and norepinephrine in mice lacking MAOA. *Science* **268**, 1763-1766.

[98] Cases O, Vitalis T, Seif I, De Maeyer E, Sotelo C, Gaspar P (1996) Lack of barrels in the somatosensory cortex of monoamine oxidase A-deficient mice: Role of a serotonin excess during the critical period. *Neuron* **16**, 297-307.

[99] Cheng A, Scott AL, Ladenheim B, Chen K, Ouyang X, Lathia JD, Mughal M, Cadet JL, Mattson MP, Shih JC (2010) Monoamine oxidases regulate telencephalic neural progenitors in late embryonic and early postnatal development. *J Neurosci* **30**, 10752-10762.

[100] Castellani RJ, Lee HG, Siedlak SL, Nunomura A, Hayashi T, Nakamura M, Zhu X, Perry G, Smith MA (2009) Reexamining Alzheimer's disease: Evidence for a protective

role for amyloid-beta protein precursor and amyloid-beta. *J Alzheimers Dis* **18**, 447-452.

[101] Hardy J (2009) The amyloid hypothesis for Alzheimer's disease: A critical reappraisal. *J Neurochem* **110**, 1129-1134.

[102] Garrick NA, Scheinin M, Chang WH, Linnoila M, Murphy DL (1984) Differential effects of clorgyline on catecholamine and indoleamine metabolites in the cerebrospinal fluid of rhesus monkeys. *Biochem Pharmacol* **33**, 1423-1427.

[103] Kitaichi Y, Inoue T, Nakagawa S, Izumi T, Koyama T (2006) Effect of co-administration of subchronic lithium pretreatment and acute MAO inhibitors on extracellular monoamine levels and the expression of contextual conditioned fear in rats. *Eur J Pharmacol* **532**, 236-245.

[104] Westlund KN, Denney RM, Rose RM, Abell CW (1988) Localization of distinct monoamine oxidase A and monoamine oxidase B cell populations in human brainstem. *Neuroscience* **25**, 439-456.

[105] Agbayewa MO (1986) Earlier psychiatric morbidity in patients with Alzheimer's disease. *J Am Geriatr Soc* **34**, 561-564.

[106] Berger AK, Fratiglioni L, Forsell Y, Winblad B, Backman L (1999) The occurrence of depressive symptoms in the preclinical phase of AD: A population-based study. *Neurology* **53**, 1998-2002.

[107] Shalat SL, Seltzer B, Pidcock C, Baker EL Jr (1987) Risk factors for Alzheimer's disease: A case-control study. *Neurology* **37**, 1630-1633.

[108] Thorpe L, Groulx B (2001) Depressive syndromes in dementia. *Can J Neurol Sci* **28**(Suppl 1), S83-S95.

[109] Kasuga K, Ohno T, Ishihara T, Miyashita A, Kuwano R, Onodera O, Nishizawa M, Ikeuchi T (2009) Depression and psychiatric symptoms preceding onset of dementia in a family with early-onset Alzheimer disease with a novel PSEN1 mutation. *J Neurol* **256**, 1351-1353.

[110] Tedde A, Forleo P, Nacmias B, Piccini C, Bracco L, Piacentini S, Sorbi S (2000) A presenilin-1 mutation (Leu392Pro) in a familial AD kindred with psychiatric symptoms at onset. *Neurology* **55**, 1590-1591.

[111] Harvey RJ, Ellison D, Hardy J, Hutton M, Roques PK, Collinge J, Fox NC, Rossor MN (1998) Chromosome 14 familial Alzheimer's disease: The clinical and neuropathological characteristics of a family with a leucine–>serine (L250S) substitution at codon 250 of the presenilin 1 gene. *J Neurol Neurosurg Psychiatry* **64**, 44-49.

[112] Mejia S, Giraldo M, Pineda D, Ardila A, Lopera F (2003) Nongenetic factors as modifiers of the age of onset of familial Alzheimer's disease. *Int Psychogeriatr* **15**, 337-349.

[113] Meyer JH, Ginovart N, Boovariwala A, Sagrati S, Hussey D, Garcia A, Young T, Praschak-Rieder N, Wilson AA, Houle S (2006) Elevated monoamine oxidase a levels in the brain: An explanation for the monoamine imbalance of major depression. *Arch Gen Psychiatry* **63**, 1209-1216.

[114] Kang DE, Yoon IS, Repetto E, Busse T, Yermian N, Ie L, Koo EH (2005) Presenilins mediate phosphatidylinositol 3-kinase/AKT and ERK activation via select signaling receptors. Selectivity of PS2 in platelet-derived growth factor signaling. *J Biol Chem* **280**, 31537-31547.

[115] Kessing LV, Sondergard L, Forman JL, Andersen PK (2009) Antidepressants and dementia. *J Affect Disord* **117**, 24-29.